



Variations in global  
methane sources and  
sinks during  
1910–2010

A. Ghosh et al.

This discussion paper is/has been under review for the journal Atmospheric Chemistry and Physics (ACP). Please refer to the corresponding final paper in ACP if available.

# Variations in global methane sources and sinks during 1910–2010

A. Ghosh<sup>1,2</sup>, P. K. Patra<sup>2,3</sup>, K. Ishijima<sup>2</sup>, T. Umezawa<sup>3,4</sup>, A. Ito<sup>2,5</sup>, D. M. Etheridge<sup>6</sup>, S. Sugawara<sup>7</sup>, K. Kawamura<sup>1,8</sup>, J. B. Miller<sup>9,10</sup>, E. J. Dlugokencky<sup>9</sup>, P. B. Krummel<sup>6</sup>, P. J. Fraser<sup>6</sup>, L. P. Steele<sup>6</sup>, R. L. Langenfelds<sup>6</sup>, J. W. C. White<sup>11</sup>, B. Vaughn<sup>11</sup>, T. Saeki<sup>2</sup>, S. Aoki<sup>3</sup>, and T. Nakazawa<sup>3</sup>

<sup>1</sup>National Institute for Polar Research, Tokyo, Japan

<sup>2</sup>Department of Environmental Geochemical Cycle Research, JAMSTEC, Yokohama, Japan

<sup>3</sup>Center for Atmospheric and Oceanic Studies, Tohoku University, Sendai, Japan

<sup>4</sup>Max-Planck Institute for Chemistry, Mainz, Germany

<sup>5</sup>National Institute for Environmental Studies, Tsukuba, Japan

<sup>6</sup>CSIRO Oceans and Atmosphere Flagship, Aspendale, Victoria, Australia

<sup>7</sup>Miyagi University of Education, Sendai, Japan

<sup>8</sup>Department of Biogeochemistry, JAMSTEC, Yokosuka, Japan

<sup>9</sup>NOAA Earth System Research Laboratory, Boulder, Colorado, USA

<sup>10</sup>CIRES, University of Colorado, Boulder, USA

<sup>11</sup>INSTAAR, University of Colorado, Boulder, Colorado, USA

Title Page

Abstract

Introduction

Conclusions

References

Tables

Figures



Back

Close

Full Screen / Esc

Printer-friendly Version

Interactive Discussion



Received: 17 October 2014 – Accepted: 17 October 2014 – Published: 5 November 2014

Correspondence to: A. Ghosh (arindamgr@gmail.com) and P. K. Patra (prabir@jamstec.go.jp)

Published by Copernicus Publications on behalf of the European Geosciences Union.

**ACPD**

14, 27619–27661, 2014

**Variations in global methane sources and sinks during 1910–2010**

A. Ghosh et al.

Title Page

Abstract

Introduction

Conclusions

References

Tables

Figures



Back

Close

Full Screen / Esc

Printer-friendly Version

Interactive Discussion



## Abstract

Atmospheric methane ( $\text{CH}_4$ ) increased from  $\sim 900$  ppb (parts per billion, or nanomoles per mole of dry air) in 1900 to  $\sim 1800$  ppb during the 2000s at a rate unprecedented in any observational records. However, the causes of the  $\text{CH}_4$  increase are poorly understood. Here we use initial emissions from bottom-up inventories for anthropogenic sources, emissions from wetlands and rice paddies simulated by a terrestrial biogeochemical model, and an atmospheric general circulation model (AGCM)-based chemistry-transport model (i.e. ACTM) to simulate atmospheric  $\text{CH}_4$  concentrations for 1910 to 2010. The ACTM simulations are compared with the  $\text{CH}_4$  concentration records reconstructed from Antarctic and Arctic ice cores and firn air samples, and from direct measurements since the 1980s at multiple sites around the globe. The differences between ACTM simulations and observed  $\text{CH}_4$  concentrations are minimized to optimize the global total emissions using a mass balance calculation. During 1910–2010, the global total  $\text{CH}_4$  emission increased from  $\sim 290 \text{ Tg yr}^{-1}$  to  $\sim 580 \text{ Tg yr}^{-1}$ . Compared to optimized emission the bottom-up emission dataset underestimates the rate of change of global total  $\text{CH}_4$  emissions by  $\sim 30\%$  during the high growth period of 1940–1990, while it overestimates by  $\sim 380\%$  during a low growth period of 1990–2010. Further, using the  $\text{CH}_4$  stable carbon isotopic data ( $\delta^{13}\text{C}$ ), we attribute the emission increase during 1940–1990 primarily to enhancement of biomass burning. The total lifetime of  $\text{CH}_4$  shortened from 9.4 yr during 1910–1919 to 9 yr during 2000–2009 by the combined effect of increasing abundance of atomic chlorine radicals (Cl) and increases in average air temperature. We show that changes of  $\text{CH}_4$  loss rate due to increased tropospheric air temperature and  $\text{CH}_4$  loss due to Cl in the stratosphere are important sources of uncertainty to more accurately estimate global  $\text{CH}_4$  budget from  $\delta^{13}\text{C}$  observations.

### Variations in global methane sources and sinks during 1910–2010

A. Ghosh et al.

Title Page

Abstract

Introduction

Conclusions

References

Tables

Figures



Back

Close

Full Screen / Esc

Printer-friendly Version

Interactive Discussion









variations such as the El Niño Southern Oscillation. Annual mean concentrations are used in this analysis, although the model integration time step is about 20 min.

## 2.2 CH<sub>4</sub> emissions

We constructed global total CH<sub>4</sub> emissions by combining: (1) the interannually varying annual mean anthropogenic emissions from the Emission Database for Global Atmospheric Research (EDGAR) – Hundred Year Database for Integrated Environmental Assessments (HYDE; version 1.4) (van Aardenne et al., 2001) and EDGAR 3.2 (Olivier and Berdowski, 2001), (2) interannually and seasonally varying emissions from rice paddies and wetland simulated by the Vegetation Integrative Simulator for Trace Gases (VISIT) terrestrial ecosystem model (Ito and Inatomi, 2012), and (3) natural emissions, such as those from biomass burning, termites based on the GISS inventory (Fung et al., 1991); emissions due to oceanic exchange near the coastal region (Lambert and Schmidt, 1993); and mud volcano emissions (Etiopie and Milkov, 2004) as the major emission components (Fig. 1a). Scaling factors for emissions due to termites, oceanic exchange, mud volcano, biomass burning, rice paddies and wetlands are 0.77, 0.40, 1.00, 0.4, 0.95, and 0.85. Scaling factors are set to simulate the CH<sub>4</sub> growth rate approximately for the first decade 1901–1910, and are in close agreement with Patra et al. (2011) for the period 1990–2008. For 1970–2000, interannually varying anthropogenic CH<sub>4</sub> emissions from EDGAR 3.2 and EDGAR 3.2FT data are used and the data have been extended for 1901–1970 following the sector-wise trends recommended in EDGAR HYDE. For 2001–2010, the EDGAR 3.2FT emissions map for 2000 is used. EDGAR 3.2 and EDGAR 3.2FT emissions for biomass burning and rice sectors (SAV, DEF, AGR, AGL sectors) are excluded from the initial CH<sub>4</sub> emissions ( $E_{ini}$ ), since they are given from different datasets as described above. The combination of different categories (Table 1) and interpolation/extrapolation of EDGAR dataset are similar to that used by Patra et al. (2011).

All of the 4 main categories of anthropogenic emissions (oil and gas, coal, animals and landfills) have increased steadily in the last 110 years; according to the EDGAR

### Variations in global methane sources and sinks during 1910–2010

A. Ghosh et al.

Title Page

Abstract

Introduction

Conclusions

References

Tables

Figures



Back

Close

Full Screen / Esc

Printer-friendly Version

Interactive Discussion





## Variations in global methane sources and sinks during 1910–2010

A. Ghosh et al.

Title Page

Abstract

Introduction

Conclusions

References

Tables

Figures

◀

▶

◀

▶

Back

Close

Full Screen / Esc

Printer-friendly Version

Interactive Discussion



5 estimated changes in Effective Equivalent tropospheric CI for the period 1992–2012 (Montzka et al., 1999; updates on the NOAA/ESRL website) and by simple extrapolation to 1901 following annual fluorocarbon production report of Alternative Fluorocarbons Environmental Acceptability Study (AFEAS) (www.afeas.org). This method ignores the changes in CI vertical distribution due to the differences in CI production rate from different species, which is altitude dependent. A delay of about 5 years between emissions of the halocarbons at Earth's surface and CI release in the stratosphere is used based on average “age” of stratospheric air in ACTM. No trends in OH are considered in this study because of lack of consensus between models, e.g., 6 out 14 models show increases in OH concentrations in the period of 1850–1980, even though the models used consistent set of anthropogenic emissions since the preindustrial era (Naik et al., 2013).

10 The time series of CH<sub>4</sub> chemical loss as calculated with ACTM simulation with  $E_{\text{ini}}$  for 1901–2010 is shown in Fig. 1b. Loss due to OH is the dominant contributor (244–466 Tgyr<sup>-1</sup>), followed by soil (18–36 Tgyr<sup>-1</sup> as simulated by the VISIT model), O(<sup>1</sup>D) (4.6–8 Tgyr<sup>-1</sup>), and Cl (1.4–15.6 Tgyr<sup>-1</sup>) over 1901–2010. Consideration of trends in Cl concentration in the ACTM results in a dramatic increase in CH<sub>4</sub> loss by Cl since the 1950s (Fig. 1b). We show later that the trends in stratospheric feedback of <sup>13</sup>C-enriched CH<sub>4</sub> cause a large imbalance in the tropospheric budget of the emission categories.

### 2.4 CH<sub>4</sub> observations: ice core/firn air data and direct measurements

The observed CH<sub>4</sub> concentrations in the Arctic and Antarctic regions were used for evaluating the ACTM simulations for two different emission scenarios. Two different types of data were used in the present study:

- 25 1. Ice core/Firn air measurements of CH<sub>4</sub> concentration – we used the Law Dome ice core records (DSS, DE08 and DE08-2) (Etheridge et al., 1998; Ferretti et al., 2005; MacFarling Meure et al., 2006) (1894–1980), and the firn records from

## Variations in global methane sources and sinks during 1910–2010

A. Ghosh et al.

Title Page

Abstract

Introduction

Conclusions

References

Tables

Figures



Back

Close

Full Screen / Esc

Printer-friendly Version

Interactive Discussion



DE08–2 (Etheridge et al., 1998) and DSSW20K (MacFarling Meure et al., 2006 and references therein) (1944–1995). The NEEM firn data<sup>1</sup> (1949–1996) are based on Buizert et al. (2012) and the NGRIP firn air data (1951–2001) are obtained from Tohoku University (Umezawa et al., unpublished data).

2. Direct atmospheric measurements from sampling networks or air archive – direct measurements of atmospheric CH<sub>4</sub> from two representative sites are used: (1) the Southern Hemisphere high latitude (Cape Grim; CGO; 40.7° S, 144.7° E) and (2) the Northern Hemisphere high latitude (Summit; SUM; 72.6° N, 38.5° W). We used station data whenever available from the NOAA Earth System Research Laboratory (NOAA/ESRL) (Dlugokencky et al., 1994); and from the Global Atmospheric Gases Experiment (GAGE) and the Advanced Global Atmospheric Gases Experiment (AGAGE) program (Prinn et al., 2000; Cunnold et al., 2002). Annual mean values are calculated from flask-based or continuous measurement data for these sites available on the World Data Centre for Greenhouse Gases (WDCGG) website (<http://ds.data.jma.go.jp/gmd/wdcgg>). The archived air samples (1978–1995) from CGO are taken from Etheridge et al. (1998).

We applied scaling factors following Dlugokencky et al. (2005), for harmonizing all data onto the Tohoku University (TU) scale (Aoki et al., 1992; Umezawa et al., 2014). It is noted that the ice core and firn air measurements have time resolution of ~5 years or more (the air age spread (1 $\sigma$ ), Etheridge et al., 1998; Trudinger et al., 2002), while the direct measurements are available at either weekly or sub-hourly time intervals. The measurement accuracy for air samples is 5 ppb or better (Etheridge et al., 1998; Umezawa et al., 2014; Dlugokencky et al., 1994; Cunnold et al., 2002). To prepare

<sup>1</sup>We apply a spline interpolation technique to calculate the age of CH<sub>4</sub> using (1) depth vs. CH<sub>4</sub> concentration and (2) CH<sub>4</sub> concentration time series data available in Buizert et al. (2012). This could be an approximate method applicable only for locked-in zone where CH<sub>4</sub> concentration monotonically decreases with depth and is less affected by diffusion of atmospheric CH<sub>4</sub>. See Buizert et al. (2012) for more accurate calculation.



Eq. (1) on the difference ( $\Delta[\text{CH}_4]$ ) between observed and simulated  $[\text{CH}_4]$ :

$$H \frac{d([\text{CH}_4])}{dt} + L = \Delta E \quad (3)$$

where  $\Delta L$  is the difference in loss terms which is calculated using  $\Delta[\text{CH}_4]$  and the ratio  $L/[\text{CH}_4]$  as a conversion factor ( $0.2907 \pm 0.0055$ ) from model simulation for individual years. The optimized emissions ( $E_{\text{opt}}$ ) are given by

$$E_{\text{opt}} = E_{\text{ini}} + \Delta E \quad (4)$$

## 2.6 Isotope analysis

The contribution of different emission categories ( $E_{\text{ini}_i}$ ) to the bottom-up emissions as used in this study is known (Fig. 1a and Table 1). However, the relative contribution of different emission categories to the emission correction  $\Delta E$  is unknown. We thus introduce an additional constraint based on  $\delta^{13}\text{C}$  for distributing  $\Delta E$  between two hypothetical source categories with lighter ( $^{13}\text{C}$ -depleted) and heavier ( $^{13}\text{C}$ -enriched) isotopic signatures.

The isotopic ratio of  $^{13}\text{C}$  to  $^{12}\text{C}$  in  $\text{CH}_4$  ( $\delta^{13}\text{C}$ ) is defined as:

$$\delta^{13}\text{C} = \left( \frac{R_{\text{sample}}}{R_{\text{std}}} - 1 \right) \times 1000 \quad (5)$$

$$R = ^{13}\text{C}/^{12}\text{C} \quad (6)$$

where  $R_{\text{sample}}$  is the isotopic molar ratio in the methane sample, and  $R_{\text{std}}$  is the corresponding ratio in the international isotope standard (Vienna Peedee Belemnite (VPDB)) with an accepted value of 0.0112372 (Craig, 1957).  $\delta^{13}\text{C}$  is expressed in “per mil” (‰) notation.

We use a one-box model (e.g., Lassey et al., 2000) to estimate the isotopic signature for global emission  $E$  ( $\delta^{13}\text{C}_E$ ) using (1) global atmospheric burden ( $B$ ) and loss

## Variations in global methane sources and sinks during 1910–2010

A. Ghosh et al.

Title Page

Abstract

Introduction

Conclusions

References

Tables

Figures

◀

▶

◀

▶

Back

Close

Full Screen / Esc

Printer-friendly Version

Interactive Discussion

( $L$ ) taken from ACTM simulation and (2) observed atmospheric isotope ratio  $\delta^{13}\text{C}_{\text{atmos}}$ . We used  $\delta^{13}\text{C}_{\text{atmos}}$  observations from the Law Dome ice core (1885–1976)/firn (1944–1998) records (Ferretti et al., 2005); from air archive samples (1978–1994) (Francey et al., 1999) and NOAA-ESRL network direct observations (1998–2010) at CGO (Miller et al., 2002; White and Vaughn, 2011). Schmitt et al. (2013) reported a possible interfering effect by Kr on  $\delta^{13}\text{C}$  measurements using continuous-flow isotope ratio mass spectrometry systems. We assume that possible bias caused by the Kr-interference is not significant in deducing the observed  $\delta^{13}\text{C}$  trends over the past century.

$\delta^{13}\text{C}_E$  can be calculated using the observed atmospheric isotope ratio  $\delta^{13}\text{C}_{\text{atmos}}$  and mass balance Eq. (1) as follows:

$${}^{13}E = \frac{d}{dt}({}^{13}B) + \sum L_i \quad (7)$$

$${}^{13}B = \left( \delta^{13}\text{C}_{\text{atmos}} \times 0.001 + 1 \right) \times R_{\text{std}} \times B \quad (8)$$

$${}^{13}L_i = L_i \times \alpha_i \times R_{\text{atmos}} \quad (9)$$

$$\delta^{13}\text{C}_E = \left[ \frac{{}^{13}E}{E \times R_{\text{std}}} - 1 \right] \times 1000 \quad (10)$$

where  $L_i$  are the loss processes due to reactions with OH, O( $^1\text{D}$ ), Cl and soil oxidation,  $\alpha_i = {}^{13}k_i / {}^{12}k_i$  is the isotopic fractionation factors for different loss processes,  $k$  is the rate coefficient of chemical reactions. Superscript 13 are used for carbon isotope  ${}^{13}\text{C}$  in  $\text{CH}_4$ .  ${}^{12}\text{CH}_4$  is approximated by  $\text{CH}_4 = {}^{12}\text{CH}_4 + {}^{13}\text{CH}_4$  excluding the more minor isotopes which has a negligible effect on our results. Our results are consistent with the calculation of  $\delta^{13}\text{C}_E$  under non-steady-state conditions (Lassey et al., 2000).

Alternatively  $\delta^{13}\text{C}_E$  can also be calculated by considering the relative fraction of individual emission categories ( $E_i$ ) as follows:

$$\delta^{13}\text{C}_E = \sum (\delta^{13}\text{C}_{E_i} \times E_i) / E \quad (11)$$

where  $E = \sum E_i$  and  $\delta^{13}\text{C}_{E_i}$  is the isotopic signature for emission category  $E_i$ . For the optimized case,  $E = E_{\text{opt}} = \sum E_{\text{ini}_i} + \Delta E$ , and  $L_i = L_{\text{opt}_i}$  and  $B = B_{\text{opt}}$  from ACTM simulation will represent the observed condition. Using Eqs. (5)–(10), we calculate the isotope signature for  $E_{\text{opt}}$  ( $\delta^{13}\text{C}_{E_{\text{opt}}}$ ). Again  $\delta^{13}\text{C}_{E_{\text{opt}}}$  can be estimated using Eq. (11) with  $E_{\text{opt}} = \sum E_{\text{ini}_i} + \Delta E$ . Here we assume that  $\Delta E$  is distributed between two hypothetical emissions  $\Delta E_l$  and  $\Delta E_h$  with lighter ( $\delta^{13}\text{C}_{\Delta E_l}$ ) and heavier ( $\delta^{13}\text{C}_{\Delta E_h}$ ) isotopic signatures, respectively. The  $\delta^{13}\text{C}_{E_i}$  are taken from Monteil et al. (2011) and references therein (Table 1). Using Eq. (11), we obtain,

$$\delta^{13}\text{C}_{E_{\text{opt}}} = \frac{\sum \delta^{13}\text{C}_{E_{\text{ini}_i}} \times E_{\text{ini}_i} + \delta^{13}\text{C}_{\Delta E_l} \times \Delta E_l + \delta^{13}\text{C}_{\Delta E_h} \times \Delta E_h}{E_{\text{opt}}} \quad (12)$$

And we have an additional constraint on  $\Delta E_l$  and  $\Delta E_h$  as follows:

$$\Delta E = \Delta E_l + \Delta E_h \quad (13)$$

The value of  $\delta^{13}\text{C}_{E_{\text{opt}}}$  as calculated using Eq. (10) is substituted into Eq. (12). There is, however, no unique solution for Eqs. (12) and (13) as they contain 4 unknown variables ( $\Delta E_h$ ,  $\Delta E_l$ ,  $\delta^{13}\text{C}_{\Delta E_h}$  and  $\delta^{13}\text{C}_{\Delta E_l}$ ). For simplicity, we assume that  $\delta^{13}\text{C}_{\Delta E_h}$  and  $\delta^{13}\text{C}_{\Delta E_l}$  represent emissions from biomass burning ( $\delta^{13}\text{C}$  is  $-21.8\%$  from Monteil et al., 2011) and residual biogenic sources (e.g., wetland, rice, animals, etc., mean  $\delta^{13}\text{C}$  near to  $-60\%$  from Sapart et al., 2012), respectively. Equation (12) can now be modified to:

$$\Delta E_l = \frac{\delta^{13}\text{C}_{E_{\text{opt}}} \times E_{\text{opt}} - \sum \delta^{13}\text{C}_{E_{\text{ini}_i}} \times E_{\text{ini}_i} - \delta^{13}\text{C}_{\Delta E_h} \times \Delta E}{(\delta^{13}\text{C}_{\Delta E_l} - \delta^{13}\text{C}_{\Delta E_h})} \quad (14)$$

27632

Variations in global methane sources and sinks during 1910–2010

A. Ghosh et al.

Title Page

Abstract

Introduction

Conclusions

References

Tables

Figures



Back

Close

Full Screen / Esc

Printer-friendly Version

Interactive Discussion



## Variations in global methane sources and sinks during 1910–2010

A. Ghosh et al.

Title Page

Abstract

Introduction

Conclusions

References

Tables

Figures



Back

Close

Full Screen / Esc

Printer-friendly Version

Interactive Discussion



Using Eq. (14) we can estimate  $\Delta E_i$  and then  $\Delta E_h$  is calculated using Eq. (13). Estimation of emissions due to biomass burning is our primary interest here because no direct statistics are available over the past century and it was assumed constant at  $49.7 \text{ Tgyr}^{-1}$  in  $E_{\text{ini}}$ . It may be reiterated here that the anthropogenic emissions varied as per the EDGAR inventories, and wetland and rice emissions are taken from a terrestrial ecosystem model simulation.

Although  $\text{CH}_4$  losses due to reactions with Cl and  $\text{O}(^1\text{D})$ , which mainly take place in the stratosphere, are small compared to the total loss, the strong isotopic fractionations ( $\varepsilon_i = (\alpha_i - 1) \times 1000$ ;  $\varepsilon_i$  is also known as “kinetic isotope effect” (KIE)) in these reactions have a large impact on the isotopic budget (Lassey et al., 2007a; Wang et al., 2002). The isotopic fractionation factors ( $\alpha_i$ ) for  $\text{CH}_4 + \text{Cl}$  reaction ( $\alpha_{\text{Cl}} = 0.935$ ) is much smaller than that of  $\text{CH}_4 + \text{OH}$  and  $\text{CH}_4 + \text{O}(^1\text{D})$  reactions, e.g.,  $\alpha_{\text{OH}} = 0.9961$  and  $\alpha_{\text{O}(^1\text{D})} = 0.9872$ , respectively (Saueressig et al., 1995). Previous studies have shown that there exists a large vertical gradient in  $\delta^{13}\text{C}$  from the troposphere to the stratosphere due to the stronger fractionations effect in  $\text{CH}_4 + \text{O}(^1\text{D})$  and  $\text{CH}_4 + \text{Cl}$  reactions during passage through the stratosphere (Rice et al., 2003; Röckmann et al., 2011; Sugawara et al., 1997). Stratosphere air returning to the troposphere is enriched in  $^{13}\text{CH}_4$ , but the re-entry flux and consequent  $^{13}\text{CH}_4$  enrichment in the troposphere are not well quantified (Lassey et al., 2007a). In a modeling study, Wang et al. (2002) estimated that the tropospheric  $^{13}\text{CH}_4$  enrichment for 1992 due to stratospheric Cl without assuming steady state was 0.23‰ (0.18–0.54‰). If the  $\alpha_i$  for Cl and  $\text{O}(^1\text{D})$  loss processes as mentioned above (Saueressig et al., 1995) are used in the one-box model, because the strong isotopic fractionations, the isotopic effect of stratospheric  $\text{CH}_4$  loss on the tropospheric  $\delta^{13}\text{C}$  budget will be overestimated. To avoid such overestimation, we assume that  $\alpha_i$  in the troposphere are mainly due to OH loss, and a smaller fractionation effect of the stratospheric loss on  $\delta^{13}\text{C}$  at the surface. In fact, the magnitude of fractionation during  $\text{CH}_4$  loss, both in the troposphere and stratosphere, is uncertain since the published values of  $\alpha_i$  in the literature are significantly different. The values of  $\alpha_{\text{Cl}}$  ranges from about 0.935 (Saueressig et al., 1995) to 0.966–0.974 (Tanaka



lations, assuming no significant uncertainties in chemistry and transport. Thus we have estimated optimized global total CH<sub>4</sub> emissions using the mass balance calculation as described in Sect. 2.5.

A new ACTM simulation using optimized emissions ( $E_{\text{opt}}$ ) was performed and the modeled CH<sub>4</sub> concentrations for the Arctic and Antarctic regions (blue and green, respectively) are shown in Fig. 2. Simulated and observed CH<sub>4</sub> are in good agreement for the ACTM using  $E_{\text{opt}}$  (see Table 2 for detailed statistics). Observations in the Antarctic region reveal that the growth rates are: moderate (5.1 ppbyr<sup>-1</sup>) during 1910–1950; fastest (13.6 ppbyr<sup>-1</sup>) during 1950–1990; moderate (6.7 ppbyr<sup>-1</sup>) during the 1990s; near-steady in the early 2000s; and moderate again (5.7 ppbyr<sup>-1</sup>) since 2007. These are all simulated well by ACTM within the measurement uncertainties of 2–5 ppb. CH<sub>4</sub> observations in the Arctic region are limited for 1949–2010. The ACTM simulated growth rates for the Arctic region follow a similar trend as the Antarctic region: 5.6 ppbyr<sup>-1</sup> during 1910–1950; 15.2 ppbyr<sup>-1</sup> during 1950–1990; 5.2 ppbyr<sup>-1</sup> during the 1990s; near-steady state during the early 2000s; and 5.8 ppbyr<sup>-1</sup> since 2007. The inter-polar difference (IPD) of CH<sub>4</sub> is, however, smaller in the model simulation (102.2 ± 17.9 ppb) compared to observations (117 ± 16.7 ppb) for the period 1949–2010. A detailed discussion on IPD is given in Sect. 3.3.

### 3.2 Trends in methane lifetime

As no consensus has been reached for the trends in global mean OH concentration simulated by state-of-the-art CTMs (e.g., John et al., 2012), we used monthly varying climatological OH concentrations for our ACTM simulations. This OH distribution, from Spivakovsky et al. (2000), also fits well with ACTM transport for simulating inter-hemispheric gradients in CH<sub>3</sub>CCl<sub>3</sub> and CH<sub>4</sub> for the period 1988–2010 (Patra et al., 2011).

For  $E_{\text{opt}}$  the total CH<sub>4</sub> lifetime is given by  $\tau_{\text{Total}} = \frac{B_{\text{opt}}}{\left(E_{\text{opt}} - \frac{dB_{\text{opt}}}{dt}\right)}$ . The trends in CH<sub>4</sub> lifetime and tropospheric mean temperature anomaly are shown in Fig. 3. The average CH<sub>4</sub> total lifetime during 1910–1919 and 2000–2009 are 9.4 ± 0.09 and 9.0 ± 0.09 years,

## Variations in global methane sources and sinks during 1910–2010

A. Ghosh et al.

Title Page

Abstract

Introduction

Conclusions

References

Tables

Figures



Back

Close

Full Screen / Esc

Printer-friendly Version

Interactive Discussion







larger the change in difference of NH-SH emissions the larger the change in IPD. The change in latitudinal distribution of emissions is the dominant driver of IPD, which is in agreement with a previous study (Mitchell et al., 2013).

### 3.4 Application of $\delta^{13}\text{C}$ for separation of source category in $\Delta E$

The difference between initial and optimized emissions ( $\Delta E = E_{\text{opt}} - E_{\text{int}}$ ) ranges from  $-15$  to  $0$  and from  $0$  to  $60 \text{ Tgyr}^{-1}$  for the first and second halves of the last 100 years, respectively (Fig. 4). Though  $E_{\text{opt}}$  reproduces the  $\text{CH}_4$  concentration for the last 100 years fairly well, it does not verify how individual source categories have evolved over the period. Here we constrain different emission categories based on evolution of  $\delta^{13}\text{C}$  by separating  $\Delta E$  into isotopically lighter and heavier sources (Sect. 2.6). We set the goal here to infer trends in emissions from biomass burning, because this emission category was kept constant over the whole simulation period due to the lack of consensus among different estimations (Mieville et al., 2010; Ito and Penner, 2005). The detailed interannual variability cannot be calculated from  $\delta^{13}\text{C}_{\text{atmos}}$  over the Antarctic region, because a smoothed fitted curve is used to interpolate between observations. For the sake of consistency, we also fitted smoothed curves for  $\delta^{13}\text{C}_{E_{\text{opt}}}$  and  $\Delta E$ , and then redistributed the smoothed  $\Delta E$  between  $\Delta E_l$  and  $\Delta E_h$ . Observations and smooth time series of  $\delta^{13}\text{C}_{\text{atmos}}$  and  $\delta^{13}\text{C}_{E_{\text{opt}}}$  are shown in Fig. 6a. We assumed  $\delta^{13}\text{C}_{\Delta E_l}$  and  $\delta^{13}\text{C}_{\Delta E_h}$  values of  $-60\text{‰}$  (representing biogenic sources) and  $-21.8\text{‰}$  (representing biomass burning emissions), respectively (Table 1). Interestingly,  $\Delta E_l$  and  $\Delta E_h$  show different trends, which indirectly illustrates the novelty of this method to provide independent pieces of information (Fig. 6b). As  $\Delta E_l$  is representing, in general, biogenic sources, a group of sources rather than an individual source, we treat it as a separate supplement source with  $\delta^{13}\text{C}_{E_l} = -60\text{‰}$ , while  $\Delta E_h$ , which represents biomass burning, an individual source, is added to the initial biomass emission ( $49.7 \text{ Tgyr}^{-1}$ ) for estimating corrected biomass burning emission ( $E_{\text{bb}} = 49.7$  (initial biomass burning emission)  $+ \Delta E_h$  (correction term)  $\text{ Tgyr}^{-1}$ ). We have taken this approach because

27638

Title Page

Abstract

Introduction

Conclusions

References

Tables

Figures



Back

Close

Full Screen / Esc

Printer-friendly Version

Interactive Discussion





## Variations in global methane sources and sinks during 1910–2010

A. Ghosh et al.

Title Page

Abstract

Introduction

Conclusions

References

Tables

Figures



Back

Close

Full Screen / Esc

Printer-friendly Version

Interactive Discussion

that of the biogenic sources in the initial emissions ( $E_{ini}$ ) for the period 1910–1980 (Fig. 1a). Between 1981–2006  $\Delta E_l$  shows a decreasing trend, followed by an increase from 2007 onward (Fig. 6b), which is different from the biogenic sources in  $E_{ini}$  showing an increasing trend during this whole period (Fig. 1a). Recent studies suggested a likely reduction in emissions from wetlands (e.g., due to more frequent El Niño events in the last three decades compared to the decades before 1980, Hodson et al., 2011, or due to the cooling effect of increased anthropogenic sulfur pollution, Gauci et al., 2004, or volcanic eruptions, Hogan et al., 1994) and changes in rice agricultural practices (Li et al., 2002). The increase in atmospheric  $CH_4$  since 2007 may be ascribed to enhanced emissions from wetlands combined with an increasing trend of fossil fuel use (Dlugokencky et al., 2009; Bousquet et al., 2011; Kirschke et al., 2013; Bergamaschi et al., 2013). Apparently,  $\Delta E_l$  is able to capture these detailed features of biogenic emissions in recent decades, which are otherwise different in  $E_{ini}$ . On the contrary, the rapid increase in emissions during 1950–1980, which is reflected in both  $\Delta E_l$  and biogenic sources in  $E_{ini}$ , is likely to be driven by increasing anthropogenic activities (e.g., agriculture, ruminants and termites, organic waste deposits etc.) related to increasing human population during this period.

The present analysis limits the unaccounted emissions  $\Delta E$  to be from only biomass burning (heavy) and biogenic (light) sources, but there could be other combinations of different categories of emissions. As we have two Eqs. (12) and (13), unique solutions are only possible for two unknown categories of emissions assuming rest of the emissions are all known. One reasonable scenario is distributing  $\Delta E$  into biomass burning and biogenic sources as examined in this study. To calculate for other possible combinations, such as fossil fuel (heavy) and biogenic (light) sources, we need to know the correct biomass burning emissions in  $E_{ini}$  and leaving the correction terms  $\Delta E_l$  and  $\Delta E_h$  erroneous. We also attempted a combination of biomass burning and fossil fuel sources, but it produced unrealistic emission values (negative). We need additional constraints such as the  $^{14}C$  (Lassey et al., 2007b) and hydrogen isotopic ratio ( $\delta D$ )



## Variations in global methane sources and sinks during 1910–2010

A. Ghosh et al.

Title Page

Abstract

Introduction

Conclusions

References

Tables

Figures

⏪

⏩

◀

▶

Back

Close

Full Screen / Esc

Printer-friendly Version

Interactive Discussion



We also estimated a supplementary biogenic source, which is likely to fill the incomplete information of biogenic sources in the initial emissions. Further details about  $\text{CH}_4$  sources could not be inferred due to limited observations covering the past 100 years and without measurements of additional constraints on  $\text{CH}_4$  source categories, such as the  $^{14}\text{C}$  and  $\delta D$ .

### Appendix A:

As the splitting of  $\Delta E$  into  $\Delta E_l$  and  $\Delta E_h$  depends on the values of  $\delta^{13}\text{C}_{\Delta E_l}$  used in the calculation, a sensitivity of estimated proposed biomass burning emission with respect to varying  $\delta^{13}\text{C}_{\Delta E_l}$ , from  $-55$  to  $-65\text{‰}$  (Sapart et al., 2012), is shown in Fig. A1. Here the estimated biomass burning emission is expressed as a decadal mean so that it is consistent with other datasets (GICC: Mieville et al., 2010; CO based reference: Ito et al., 2005). The uncertainty in estimation of possible biomass burning emissions increases from 1950 onward reaching a peak in 1990s.

*Acknowledgements.* This research is financially supported by the Green Network of Excellence (GRENE) Project by the Ministry of Education, Culture, Sports, Science and Technology (MEXT), Japan. We also acknowledge data centers/contributors Tohoku University, Japan; NOAA/ESRL air sampling network; GAGE/AGAGE network; NOAA's National Climate Data Center (NCDC); World Data Centre for Greenhouse Gases (WDCGG); Carbon Dioxide Information Analysis Center (CDIAC), U.S. Department of Energy; the Australian Bureau of Meteorology/Cape Grim Baseline Air Pollution Station; Commonwealth Scientific and Industrial Research Organisation (CSIRO), Australia for the dataset used in the present study. CSIRO's contribution was supported in part by the Australian Climate Change Science Program, an Australian Government Initiative.

## References

- Aoki, S., Nakazawa, T., Murayama, S., and Kawaguchi, S.: Measurements of atmospheric methane at the Japanese Antarctic Station, Syowa, *Tellus B*, 44, 273–281, 1992.
- Baumgartner, M., Schilt, A., Eicher, O., Schmitt, J., Schwander, J., Spahni, R., Fischer, H., and Stocker, T. F.: High-resolution inter-polar difference of atmospheric methane around the Last Glacial Maximum, *Biogeosciences*, 9, 3961–3977, doi:10.5194/bg-9-3961-2012, 2012.
- Bergamaschi P., Houweling, S., Segers, A., Krol, M., Frankenberg, C., Scheepmaker, R., Dlugokencky, E., Wofsy, S., Kort, E., Sweeney, C., Schuck, T., Brenninkmeijer, C., Chen, H., Beck, V., and Gerbig, C.: Atmospheric CH<sub>4</sub> in the first decade of the 21st century: inverse modeling analysis using SCIAMACHY satellite retrievals and NOAA surface measurements, *J. Geophys. Res.-Atmos.*, 118, 7350–7369, doi:10.1002/jgrd.50480, 2013.
- Bousquet, P., Ciais, P., Miller, J. B., Dlugokencky, E. J., Hauglustaine, D. A., Prigent, C., Van der Werf, G. R., Peylin, P., Brunke, E. G., Carouge, C., Langenfelds, R. L., Lathiere, J., Papa, F., Ramonet, M., Schmidt, M., Steele, L. P., Tyler, S. C., and White, J.: Contribution of anthropogenic and natural sources to atmospheric methane variability, *Nature*, 443, 439–443, doi:10.1038/nature05132, 2006.
- Bousquet, P., Ringeval, B., Pison, I., Dlugokencky, E. J., Brunke, E.-G., Carouge, C., Chevalier, F., Fortems-Cheiney, A., Frankenberg, C., Hauglustaine, D. A., Krummel, P. B., Langenfelds, R. L., Ramonet, M., Schmidt, M., Steele, L. P., Szopa, S., Yver, C., Viovy, N., and Ciais, P.: Source attribution of the changes in atmospheric methane for 2006–2008, *Atmos. Chem. Phys.*, 11, 3689–3700, doi:10.5194/acp-11-3689-2011, 2011.
- Buizert, C., Martinerie, P., Petrenko, V. V., Severinghaus, J. P., Trudinger, C. M., Witrant, E., Rosen, J. L., Orsi, A. J., Rubino, M., Etheridge, D. M., Steele, L. P., Hogan, C., Laube, J. C., Sturges, W. T., Levchenko, V. A., Smith, A. M., Levin, I., Conway, T. J., Dlugokencky, E. J., Lang, P. M., Kawamura, K., Jenk, T. M., White, J. W. C., Sowers, T., Schwander, J., and Blunier, T.: Gas transport in firn: multiple-tracer characterisation and model intercomparison for NEEM, Northern Greenland, *Atmos. Chem. Phys.*, 12, 4259–4277, doi:10.5194/acp-12-4259-2012, 2012.
- Cantrell, C. A., Shetter, R. E., McDaniel, A. H., Calvert, J. G., Davidson, J. A., Lowe, D. C., Tyler, S. C., Cicerone, R. J., and Greenberg, J. P.: Carbon kinetic isotope effect in the oxidation of methane by hydroxyl radicals, *J. Geophys. Res.*, 95, 22455–22462, 1990.

## Variations in global methane sources and sinks during 1910–2010

A. Ghosh et al.

Title Page

Abstract

Introduction

Conclusions

References

Tables

Figures



Back

Close

Full Screen / Esc

Printer-friendly Version

Interactive Discussion



**Variations in global methane sources and sinks during 1910–2010**

A. Ghosh et al.

Title Page

Abstract

Introduction

Conclusions

References

Tables

Figures



Back

Close

Full Screen / Esc

Printer-friendly Version

Interactive Discussion



Cao, M., Gregson, K., and Marshall, S.: Global methane emission from wetlands and its sensitivity to climate change, *Atmos. Environ.*, 32, 3293–3299, doi:10.1016/S1352-2310(98)00105-8, 1998.

Chappellaz, J. A., Fung, I. Y., and Thompson, A. M.: The atmospheric CH<sub>4</sub> increase since the last glacial maximum, 1, *Source estimates*, *Tellus B*, 45, 228–241, 1993.

Cicerone, R. J. and Oremland, R. S.: Biogeochemical aspects of atmospheric methane, *Global Biogeochem. Cy.*, 2, 299–327, 1988.

Craig, H.: Isotopic standards for carbon and oxygen and correction factors for mass spectrometric analysis of carbon dioxide, *Geochim. Cosmochim. Ac.*, 12, 133–149, 1957.

Cunnold, D. M., Steele, L. P., Fraser, P. J., Simmonds, P. G., Prinn, R. G., Weiss, R. F., Porter, L. W., O'Doherty, S., Langenfelds, R. L., Krummel, P. B., Wang, H. J., Emmons, L., Tie, X. X., and Dlugokencky, E. J.: In situ measurements of atmospheric methane at GAGE/AGAGE sites during 1985–2000 and resulting source inferences, *J. Geophys. Res.-Atmos.*, 107, 4225, doi:10.1029/2001JD001226, 2002.

Davidson, J. A., Cantrell, C. A., Tyler, S. C., Shetter, R. E., Cicerone, R. J., and Calvert, J. G.: Carbon kinetic isotope effect in the reaction of CH<sub>4</sub> with HO, *J. Geophys. Res.*, 92, 2195–2199, 1987.

Dlugokencky, E. J., Masarie, K. A., Lang, P. M., Tans, P. P., Steele, L. P., and Nisbet, E. G.: A dramatic decrease in the growth rate of atmospheric methane in the Northern Hemisphere during 1992, *Geophys. Res. Lett.*, 21, 45–48, 1994.

Dlugokencky, E. J., Houweling, S., Bruhwiler, L., Masarie, K. A., Lang, P. M., Miller, J. B., and Tans, P. P.: Atmospheric methane levels off: temporary pause or a new steady-state?, *Geophys. Res. Lett.*, 30, 1992, doi:10.1029/2003GL018126, 2003.

Dlugokencky, E. J., Myers, R. C., Lang, P. M., Masarie, K. A., Crotwell, A. M., Thoning, K. W., Hall, B. D., Elkins, J. W., and Steele, L. P.: Conversion of NOAA atmospheric dry air CH<sub>4</sub> mole fractions to a gravimetrically prepared standard scale, *J. Geophys. Res.*, 110, D18306, doi:10.1029/2005JD006035, 2005.

Dlugokencky, E. J., Bruhwiler, L., White, J. W. C., Emmons, L. K., Novelli, P. C., Montzka, S. A., Masarie, K. A., Lang, P. M., Crotwell, A. M., Miller, J. B., and Gatti, L. V.: Observational constraints on recent increases in the atmospheric CH<sub>4</sub> burden, *Geophys. Res. Lett.*, 36, L18803, doi:10.1029/2009GL039780, 2009.

Dlugokencky, E. J., Nisbet, E. G., Fisher, R., and Lowry, D.: Global atmospheric methane: budget, changes and dangers, *Philos. T. R. Soc. A*, 369, 2058–2072, 2011.

**Variations in global methane sources and sinks during 1910–2010**

A. Ghosh et al.

Title Page

Abstract

Introduction

Conclusions

References

Tables

Figures



Back

Close

Full Screen / Esc

Printer-friendly Version

Interactive Discussion



Etheridge, D. M., Steele, L. P., Francey, R. J., and Langenfelds, R. L.: Atmospheric methane between 1000 A. D., and present: evidence of anthropogenic emissions and climatic variability, *J. Geophys. Res.*, 103, 15979–15993, doi:10.1029/98JD00923, 1998.

5 Etiope, G. and Milkov, A. V.: A new estimate of global methane flux from onshore and shallow submarine mud volcanoes to the atmosphere, *Environ. Geol.*, 46, 997–1002, doi:10.1007/s00254-004-1085-1, 2004.

Ferretti, D. F., Miller, J. B., White, J. W. C., Etheridge, D. M., Lassey, K. R., Lowe, D. C., MacFarling Meure, C. M., Dreier, M. F., Trudinger, C. M., van Ommen, T. D., and Langenfelds, R. L.: Unexpected changes to the global methane budget over the past 2000 years, *Science*, 309, 1714–1717, doi:10.1126/science.1115193, 2005.

10 Francey, R. J., Manning, M. R., Allison, C. E., Coram, S. A., Etheridge, D. M., Langenfelds, R. L., Lowe, D. C., and Steele, L. P.: A history of  $\delta^{13}\text{C}$  in atmospheric  $\text{CH}_4$  from the Cape Grim Air Archive and Antarctic firn air, *J. Geophys. Res.*, 104, 23631–23643, doi:10.1029/1999JD900357, 1999.

15 Fung, I., John, J., Lerner, J., Matthews, E., Prather, M., Steele, L. P., and Fraser, P. J.: Three-dimensional model synthesis of the global methane cycle, *J. Geophys. Res.*, 96, 13033–13065, doi:10.1029/91JD01247, 1991.

Gauci V, Matthews, E., Dise, N., Walter, B., Koch, D., Granberg, G., and Vile, M. A.: Sulfur pollution suppression of the wetland methane source in the 20th and 21st centuries, *Proc. Natl. Acad. Sci. USA* 101, 12583–12587, 2004.

20 Gupta, M. L., McGrath, M. P., Cicerone, R. J., Rowland, F. S., and Wolfsberg, M.:  $^{12}\text{C}/^{13}\text{C}$  kinetic isotope effects in the reactions of  $\text{CH}_4$  with OH and Cl, *Geophys. Res. Lett.*, 24, 2761–2764, 1997.

Hansen, J., Ruedy, R., Sato, M., and Lo, K.: Global surface temperature change, *Rev. Geophys.*, 48, RG4004, doi:10.1029/2010RG000345, 2010.

25 Hodson, E. L., Poulter, B., Zimmermann, N. E., Prigent, C., and Kaplan, J. O.: The El Niño–Southern Oscillation and wetland methane interannual variability, *Geophys. Res. Lett.*, 38, L08810, doi:10.1029/2011GL046861, 2011.

Hogan, K. B. and Harriss, R. C.: Comment on “A dramatic decrease in the growth rate of atmospheric methane in the Northern Hemisphere during 1992” by E. J. Dlugokencky et al., *Geophys. Res. Lett.*, 21, 2445–2446, doi:10.1029/94GL02601, 1994.

5

10

15

20

25

30





## Variations in global methane sources and sinks during 1910–2010

A. Ghosh et al.

[Title Page](#)[Abstract](#)[Introduction](#)[Conclusions](#)[References](#)[Tables](#)[Figures](#)[Back](#)[Close](#)[Full Screen / Esc](#)[Printer-friendly Version](#)[Interactive Discussion](#)

- Mitchell, L., Brook, E., Lee, J. E., Buizert, C., and Sowers, T.: Constraints on the Late Holocene anthropogenic contribution to the atmospheric methane budget, *Science*, 22, 964–966, doi:10.1126/science.1238920, 2013.
- Montiel, C. and Kraus, D. (Eds.): *Best Practices of Fire Use: Prescribed Burning and Suppression: Fire Programmes in Selected Case-study Regions in Europe*, European Forest Institute, WS Bookwell Oy, Porvoo, Finland, Report 24, 169 pp., 2010.
- Monteil, G., Houweling, S., Dlugokenky, E. J., Maenhout, G., Vaughn, B. H., White, J. W. C., and Rockmann, T.: Interpreting methane variations in the past two decades using measurements of CH<sub>4</sub> mixing ratio and isotopic composition, *Atmos. Chem. Phys.*, 11, 9141–9153, doi:10.5194/acp-11-9141-2011, 2011.
- Montzka, S. A., Butler, J. H., Elkins, J. W., Thompson, T. M., Clarke, A. D., and Lock, L. T.: Present and future trends in the atmospheric burden of ozone-depleting halogens, *Nature*, 398, 690–694, 1999.
- Myhre, G., Shindell, D., Bréon, F.-M., Collins, W., Fuglestad, J., Huang, J., Koch, D., Lamarque, J.-F., Lee, D., Mendoza, B., Nakajima, T., Robock, A., Stephens, G., Takemura, T., and Zhang, H.: Anthropogenic and natural radiative forcing, in: *Climate Change 2013: The Physical Science Basis*, Fifth Assessment Report of the Intergovernmental Panel on Climate Change, edited by: Stocker, T. F. et al., Cambridge University Press, Cambridge, UK, New York, NY, USA, 659–740, 2013.
- Naik, V., Voulgarakis, A., Fiore, A. M., Horowitz, L. W., Lamarque, J.-F., Lin, M., Prather, M. J., Young, P. J., Bergmann, D., Cameron-Smith, P. J., Cionni, I., Collins, W. J., Dalsøren, S. B., Doherty, R., Eyring, V., Faluvegi, G., Folberth, G. A., Josse, B., Lee, Y. H., MacKenzie, I. A., Nagashima, T., van Noije, T. P. C., Plummer, D. A., Righi, M., Rumbold, S. T., Skeie, R., Shindell, D. T., Stevenson, D. S., Strode, S., Sudo, K., Szopa, S., and Zeng, G.: Preindustrial to present-day changes in tropospheric hydroxyl radical and methane lifetime from the Atmospheric Chemistry and Climate Model Intercomparison Project (ACCMIP), *Atmos. Chem. Phys.*, 13, 5277–5298, doi:10.5194/acp-13-5277-2013, 2013.
- Nakazawa, T., Machida, T., Tanaka, M., Fujii, Y., Aoki, S., and Watanabe, O.: Differences of the atmospheric CH<sub>4</sub> concentration between the Arctic and Antarctic regions in pre-industrial/pre-agricultural era, *Geophys. Res. Lett.*, 20, 943–946, 1993.
- Olivier, J. G. J. and J. J. M.: Global emissions sources and sinks, in: *The Climate System*, edited by: Berdowski, J., Guicherit, R., and Heij, B. J., A. A. Balkema Publishers/Swets & Zeitlinger Publishers, Lisse, the Netherlands, ISBN 9058092550, 33–78, 2001.

## Variations in global methane sources and sinks during 1910–2010

A. Ghosh et al.

Title Page

Abstract

Introduction

Conclusions

References

Tables

Figures



Back

Close

Full Screen / Esc

Printer-friendly Version

Interactive Discussion



Onogi, K., Tsutsui, J., Koide, H., Sakamoto, M., Kobayashi, S., Hatsushika, H. Matsumoto, T., Yamazaki, N., Kamahori, H., Takahashi, K., Kadokura, S., Wada, K., Kato, K., Oyama, R., Ose, T., Mannoji, N., and Taira, R.: The JRA-25 reanalysis, *J. Meteorol. Soc. Jpn.*, 85, 369–432, 2007.

5 Patra, P. K., Takigawa, M., Dutton, G. S., Uhse, K., Ishijima, K., Lintner, B. R., Miyazaki, K., and Elkins, J. W.: Transport mechanisms for synoptic, seasonal and interannual SF<sub>6</sub> variations and "age" of air in troposphere, *Atmos. Chem. Phys.*, 9, 1209–1225, doi:10.5194/acp-9-1209-2009, 2009.

10 Patra, P. K., Houweling, S., Krol, M., Bousquet, P., Belikov, D., Bergmann, D., Bian, H., Cameron-Smith, P., Chipperfield, M. P., Corbin, K., Fortems-Cheiney, A., Fraser, A., Gloor, E., Hess, P., Ito, A., Kawa, S. R., Law, R. M., Loh, Z., Maksyutov, S., Meng, L., Palmer, P. I., Prinn, R. G., Rigby, M., Saito, R., and Wilson, C.: TransCom model simulations of CH<sub>4</sub> and related species: linking transport, surface flux and chemical loss with CH<sub>4</sub> variability in the troposphere and lower stratosphere, *Atmos. Chem. Phys.*, 11, 12813–12837, doi:10.5194/acp-11-12813-2011, 2011.

15 Patra, P. K., Ito, A., and Yan, X.: Climate change and agriculture in Asia: a case study for methane emission due to rice cultivation, in: *Climate Change and Agriculture*, edited by: Bhattacharyya, T., Pal, D. K., Sarkar, D., and Wani, S. P., Studium press (India) Pvt. Ltd., New Delhi, ISBN978-93-80012-40-7, 328 pp., 2013.

20 Prinn, R. G., Weiss, R. F., Fraser, P. J., Simmonds, P. G., Cunnold, D. M., Alyea, F. N., O'Doherty, S., Salameh, P., Miller, B. R., Huang, J., Wang, R. H. J., Hartley, D. E., Harth, C., Steele, L. P., Sturrock, G., Midgley, P. M., and McCulloch, A.: A history of chemically and radiatively important gases in air deduced from ALE/GAGE/AGAGE, *J. Geophys. Res.*, 105, 17751–17792, doi:10.1029/2000JD900141, 2000.

25 Quay, P., Stutsman, J., Wilbur, D., Snover, A., Dlugokencky, E., and Brown, T.: The isotopic composition of atmospheric methane, *Global Biogeochem. Cy.*, 13, 445–461, doi:10.1029/1998GB900006, 1999.

Rasmussen, R. A. and Khalil, M. A. K.: Atmospheric methane in the recent and ancient atmospheres: concentrations, trends, and interhemispheric gradient, *J. Geophys. Res.*, 89, 11599–11605, doi:10.1029/JD089iD07p11599, 1984.

30 Rayner, N. A., Parker, D. E., Horton, E. B., Folland, C. K., Alexander, L. V., Rowell, D. P., Kent, E. C., and Kaplan, A.: Global analyses of sea surface temperature, sea ice, and

**Variations in global methane sources and sinks during 1910–2010**

A. Ghosh et al.

Title Page

Abstract

Introduction

Conclusions

References

Tables

Figures



Back

Close

Full Screen / Esc

Printer-friendly Version

Interactive Discussion



night marine air temperature since the late nineteenth century, *J. Geophys. Res.*, 108, 4407 doi:10.1029/2002JD002670, 2003.

Rigby, M., Prinn, R. G., Fraser, P. J., Simmonds, P. G., Langenfelds, R. L., Huang, J., Cunnold, D. M., Steele, L. P., Krummel, P. B., Weiss, R. F., O'Doherty, S., Salameh, P. K., Wang, H. J., Harth, C. M., Mühle, J., and Porter, L. W.: Renewed growth of atmospheric methane, *Geophys. Res. Lett.*, 35, L22805, doi:10.1029/2008GL036037, 2008.

Rice, A. L., Tyler, S. C., McCarthy, M. C., Boering, K. A., and Atlas, E.: Carbon and hydrogen isotopic compositions of stratospheric methane: 1. High-precision observations from the NASA ER-2 aircraft, *J. Geophys. Res.*, 108, 4460, doi:10.1029/2002JD003042, 2003.

Röckmann, T., Brass, M., Borchers, R., and Engel, A.: The isotopic composition of methane in the stratosphere: high-altitude balloon sample measurements, *Atmos. Chem. Phys.*, 11, 13287–13304, doi:10.5194/acp-11-13287-2011, 2011.

Sander, S. P., Friedl, R. R., Golden, D. M., Kurylo, M. J., Moortgat, G. K., Keller-Rudek, H., Wine, P. H., Ravishankara, A. R., Kolb, C. E., Molina, M. J., Finlayson-Pitts, B. J., Huie, R. E., and Orkin, V. L.: Chemical Kinetics and Photochemical Data for Use in Atmospheric Studies, Evaluation Number 15, JPL Publication 06-2, Jet Propulsion Laboratory, Pasadena, CA, 2006.

Sapart, C. J., Monteil, G., Prokopiou, M., Van de Wal, R. S. W., Kaplan, J. O., Sperlich, P., Krumhardt, K. M., Van der Veen, C., Houweling, S., Krol, M. C., Blunier, T., Sowers, T., Martinerie, P., Witrant, E., Dahl-Jensen, D., and Röckmann, T.: Natural and anthropogenic variations in methane sources during the past two millennia, *Nature*, 490, 85–88, doi:10.1038/nature11461, 2012.

Sapart, C. J., Martinerie, P., Witrant, E., Chappellaz, J., van de Wal, R. S. W., Sperlich, P., van der Veen, C., Bernard, S., Sturges, W. T., Blunier, T., Schwander, J., Etheridge, D., and Röckmann, T.: Can the carbon isotopic composition of methane be reconstructed from multi-site firn air measurements?, *Atmos. Chem. Phys.*, 13, 6993–7005, doi:10.5194/acp-13-6993-2013, 2013.

Sathaye, J. and Tyler, S.: Transitions in household energy use in urban China, India, the Philippines, Thailand and Hong Kong, *Annu. Rev. Energ. Env.*, 16, 295–335, 1991.

Saueressig, G., Bergamaschi, P., Crowley, J. N., Fischer, H., and Harris, G. W.: Carbon kinetic isotope effect in the reaction of CH<sub>4</sub> With Cl atoms, *Geophys. Res. Lett.*, 22, 1225–1228, 1995.

**Variations in global methane sources and sinks during 1910–2010**

A. Ghosh et al.

Title Page

Abstract

Introduction

Conclusions

References

Tables

Figures

◀

▶

◀

▶

Back

Close

Full Screen / Esc

Printer-friendly Version

Interactive Discussion



- Saueressig, G., Crowley, J. N., Bergamaschi, P., Bruhl, C., Brenninkmeijer, C. A. M., and Fischer, H.: Carbon 13 and D kinetic isotope effects in the reactions of CH<sub>4</sub> with O(<sup>1</sup>D) and OH: new laboratory measurements and their implications for the isotopic composition of stratospheric methane, *J. Geophys. Res.*, 106, 23127–23138, 2001.
- 5 Schmitt, J., Seth, B., Bock, M., van der Veen, C., Möller, L., Sapart, C. J., Prokopiou, M., Sowers, T., Röckmann, T., and Fischer, H.: On the interference of Kr during carbon isotope analysis of methane using continuous-flow combustion–isotope ratio mass spectrometry, *Atmos. Meas. Tech.*, 6, 1425–1445, doi:10.5194/amt-6-1425-2013, 2013.
- 10 Spivakovsky, C. M., Logan, J. A., Montzka, S. A., Balkanski, Y. J., Foreman-Fowler, M., Jones, D. B. A., Horowitz, L. W., Fusco, A. C., Brenninkmeijer, C. A. M., Prather, M. J., Wofsy, S. C., and McElroy, M. B.: Three-dimensional climatological distribution of tropospheric OH: update and evaluation, *J. Geophys. Res.*, 105, 8931–8980, doi:10.1029/1999JD901006, 2000.
- 15 Sugawara, S., Nakazawa, T., Shirakawa, Y., Kawamura, K., and Aoki, S.: Vertical profile of the carbon isotopic ratio of stratospheric methane over Japan, *Geophys. Res. Lett.*, 24, 2989–2992, 1997.
- Tanaka, N., Xiao, Y., and Lasaga, A. C.: Ab initio study on carbon kinetic isotope effect (KIE) in the reaction of CH<sub>4</sub> + Cl, *J. Atmos. Chem.*, 23, 37–49, 1996.
- 20 Takigawa, M., Takahashi, M., and Akiyoshi, H.: Simulation of ozone and other chemical species using a Center for Climate System Research/National Institute for Environmental Studies atmospheric GCM with coupled stratospheric chemistry, *J. Geophys. Res.*, 104, 14003–14018, 1999.
- Trudinger, C. M., Enting, I. G., Rayner, P. J., and Francey, R. J.: Kalman filter analysis of ice core data, 2. Double deconvolution of CO<sub>2</sub> and δ<sup>13</sup>C measurements, *J. Geophys. Res.*, 107, 4423, doi:10.1029/2001JD001112, 2002.
- 25 Umezawa, T., Goto, D., Aoki, S., Ishijima, K., Patra, P. K., Sugawara, S., Morimoto, S., and Nakazawa, T.: Variations of tropospheric methane over Japan during 1988–2010, *Tellus B*, 66, 23837, doi:10.3402/tellusb.v66.23837, 2014.
- 30 van Aardenne, J. A., Dentener, F. J., Olivier, J. G. J., Klein Goldewijk, C. G. M., and Lelieveld, J.: A high resolution dataset of historical anthropogenic trace gas emissions for the period 1890–1990, *Global Biogeochem. Cy.*, 15, 909–928, 2001.

Wang, J. S., McElroy, M. B., Spivakovsky, C. M., and Jones, D. B. A.: On the contribution of anthropogenic Cl to the increase in  $d^{13}C$  of atmospheric methane, *Global Biogeochem. Cy.*, 16, 1047, doi:10.1029/2001GB001572, 2002.

5 White, J. W. C. and Vaughn, B. H.: University of Colorado, Institute of Arctic Alpine Research (INSTAAR), Stable Isotopic Composition of Atmospheric Methane ( $^{13}C$ ) from the NOAA ESRL Carbon Cycle Cooperative Global Air Sampling Network, 1998–2011, Version: 2013-04-05, available at: ftp://ftp.cmdl.noaa.gov/ccg/ch4c13/flask/event/ (last access: 5 April 2013), 2011.

Variations in global methane sources and sinks during 1910–2010

A. Ghosh et al.

Title Page

Abstract

Introduction

Conclusions

References

Tables

Figures



Back

Close

Full Screen / Esc

Printer-friendly Version

Interactive Discussion



**Table 1.** Average source and sink strengths of CH<sub>4</sub> for 1980–1989, isotopic ratios ( $\delta^{13}\text{C}_{E_i}$ ) and fractionation factors ( $\alpha_i$ ).

Source/Sink	Annual Flux (Tgyr <sup>-1</sup> )	$\delta^{13}\text{C}_{E_i}$ (‰)	$\alpha_i^a$
<b>Sources</b>			
Wetland	146.8	-59	
Rice	34.2	-63	
Animals	83.5	-62	
Termites	20.7	-57	
Biomass Burning	49.7	-21.8	
Coal	30.6	-35	
Oil and Gas	59.2	-40	
Landfills	46.0	-55	
Ocean	7.4	-59	
Mud Volcanoes	7.5	-40	
$\Delta E^b$	60.0	-21.8	
		-60.0	
<hr/>			
Total Source	545.6		
<hr/>			
<b>Sinks</b>			
OH	-451.5		0.995350
O(1D)	-7.5		0.994940
Cl	-14.5		0.992532
Soil	-28.6		0.978000
<hr/>			
Total Sinks	-502.1		

<sup>a</sup>  $\alpha_{\text{OH}}$  is the mean of two published values (Cantrell et al., 1990; Saueressig et al., 2001), while the values of  $\alpha_{\text{Cl}}$  and  $\alpha_{\text{O}(1\text{D})}$  are modified assuming the smaller effect of isotopic fractionation in the stratosphere at the surface.

<sup>b</sup>  $\Delta E$  is assumed to consist of isotopically heavier ( $\delta^{13}\text{C} = -21.8\%$ ) and lighter ( $\delta^{13}\text{C} = -60\%$ ) sources.

## Variations in global methane sources and sinks during 1910–2010

A. Ghosh et al.

**Table 2.** Average bias and 1 SD (in ppb) of model-observed CH<sub>4</sub> concentration for each decade over the Antarctic region. The averages of  $E_{ini}$ ,  $E_{opt}$  and  $B_{opt}$  for each decade are also shown.

Decade	Model-observation CH <sub>4</sub> concentration (ppb)		$E_{ini}$ (Tgyr <sup>-1</sup> )	$E_{opt}$ (Tgyr <sup>-1</sup> )	$B_{opt}$ (Tg)
	with $E_{ini}$	with $E_{opt}$			
1910–1919	40.94 ± 3.29	-3.31 ± 0.51	315.0	300.1	2686.4
1920–1929	37.33 ± 5.30	-2.07 ± 0.37	326.4	319.9	2846.7
1930–1939	21.21 ± 3.25	-0.44 ± 0.67	337.0	334.1	3002.7
1940–1949	13.92 ± 1.85	0.05 ± 0.39	351.2	349.2	3132.0
1950–1959	0.13 ± 6.84	-0.61 ± 0.44	375.7	381.9	3331.7
1960–1969	-38.96 ± 16.31	0.11 ± 1.26	407.2	434.4	3675.5
1970–1979	-101.88 ± 20.66	-1.04 ± 0.75	442.4	491.6	4109.6
1980–1989	-160.65 ± 14.15	0.15 ± 1.59	485.6	545.6	4572.7
1990–1999	-161.76 ± 8.37	2.54 ± 2.12	515.0	557.8	4878.8
2000–2009	-122.40 ± 15.34	2.67 ± 3.25	531.0	555.0	4973.2

Title Page

Abstract

Introduction

Conclusions

References

Tables

Figures

◀

▶

◀

▶

Back

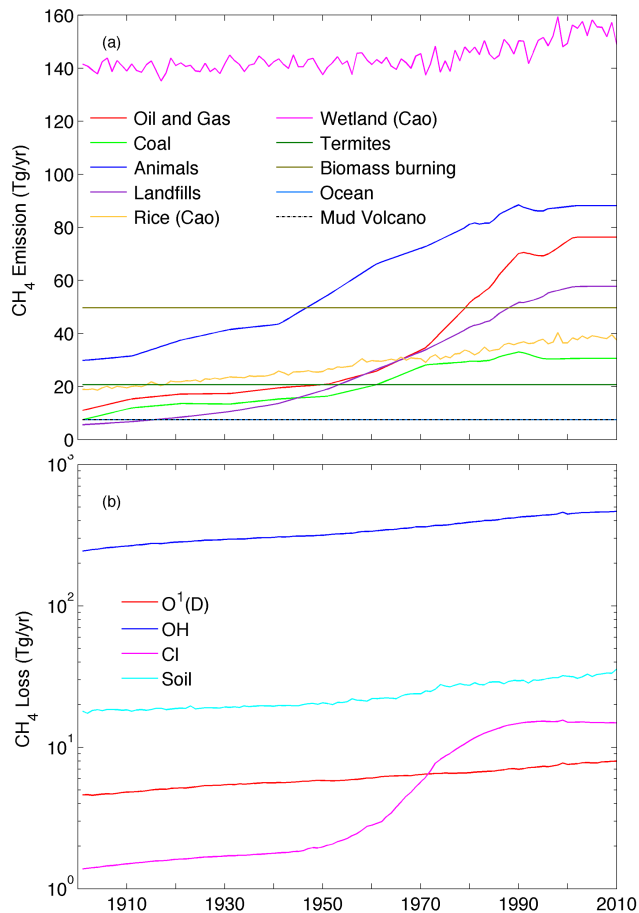
Close

Full Screen / Esc

Printer-friendly Version

Interactive Discussion

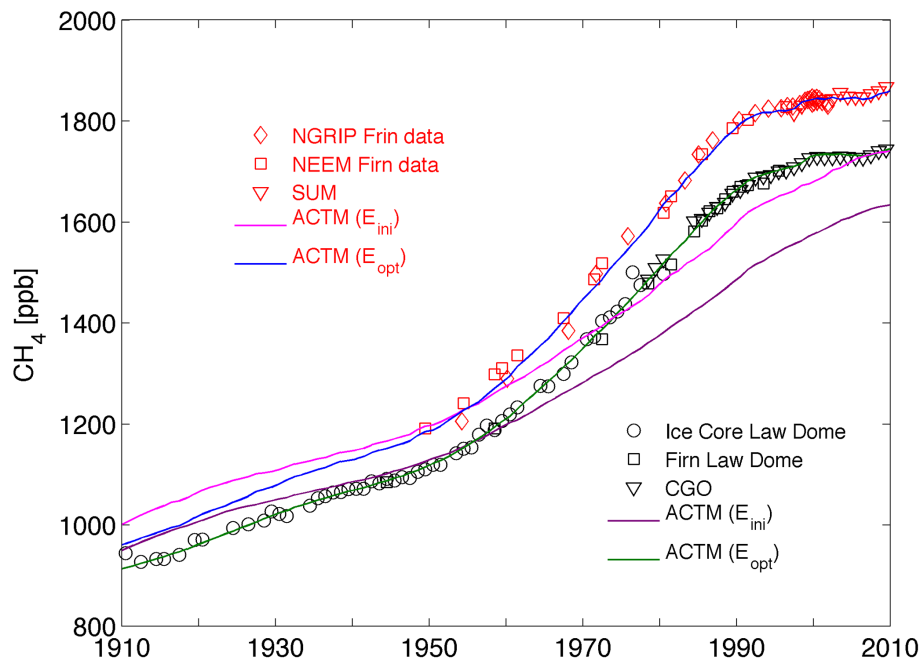




**Figure 1.** (a) Time series of CH<sub>4</sub> emission inventory estimates from different categories during our simulation. (b) Chemical loss of CH<sub>4</sub> calculated using ACTM simulation with initial emissions ( $E_{ini}$ ).

## Variations in global methane sources and sinks during 1910–2010

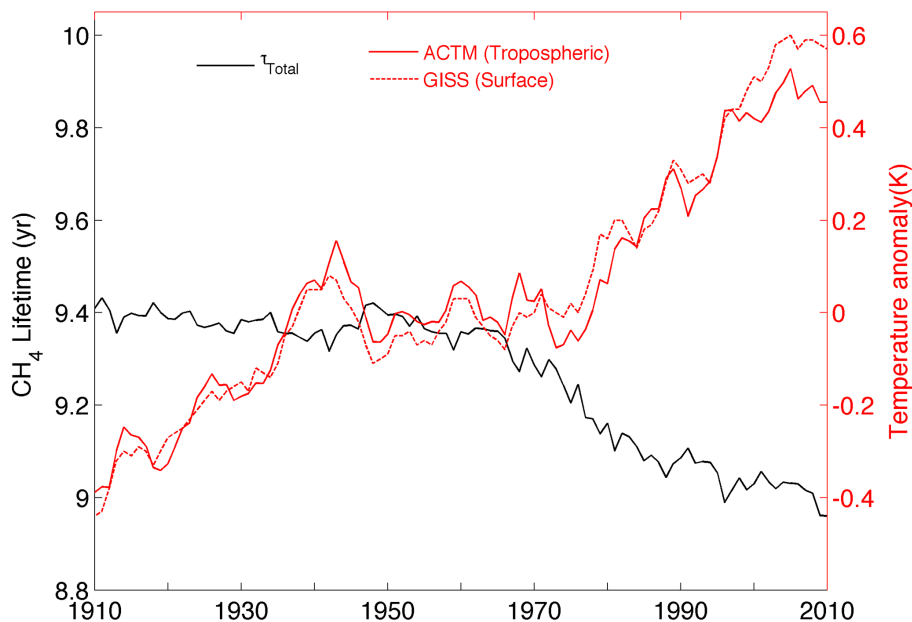
A. Ghosh et al.



**Figure 2.** ACTM simulations of  $\text{CH}_4$  concentration compared with ice core, firn and direct measurements. ACTM simulated  $\text{CH}_4$  concentrations with  $E_{\text{ini}}$  ( $E_{\text{opt}}$ ) for Arctic and Antarctic regions are shown in magenta (blue) and purple (green), respectively. Red (black) symbol and text are for Arctic (Antarctic) region. Annual average ice core data (Law Dome: DSS, DE08 and DE08-2), firn records (Law Dome (DE08-2 and DSSW20K); NGRIP firn data; and NEEM firn data) and direct observations (CGO: air archive, flask sampling and GAGE/AGAGE; SUM: flask sampling) are prepared and presented separately here. All the observation data are referenced to the Tohoku University (TU)  $\text{CH}_4$  scale (Aoki et al., 1992; Umezawa et al., 2014).

## Variations in global methane sources and sinks during 1910–2010

A. Ghosh et al.

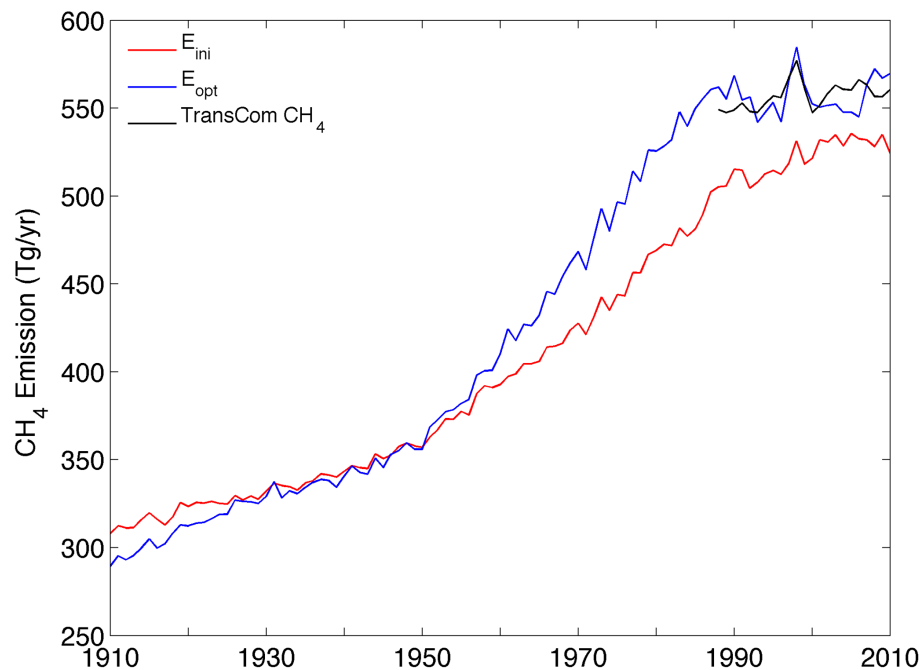


**Figure 3.** Five-year running means of CH<sub>4</sub> total lifetime and global tropospheric temperature anomaly (with the base period 1951–1980) during 1910–2010.

[Title Page](#)[Abstract](#)[Introduction](#)[Conclusions](#)[References](#)[Tables](#)[Figures](#)[◀](#)[▶](#)[◀](#)[▶](#)[Back](#)[Close](#)[Full Screen / Esc](#)[Printer-friendly Version](#)[Interactive Discussion](#)

## Variations in global methane sources and sinks during 1910–2010

A. Ghosh et al.

[Title Page](#)[Abstract](#)[Introduction](#)[Conclusions](#)[References](#)[Tables](#)[Figures](#)[◀](#)[▶](#)[◀](#)[▶](#)[Back](#)[Close](#)[Full Screen / Esc](#)[Printer-friendly Version](#)[Interactive Discussion](#)

**Figure 4.** Time series of initial ( $E_{ini}$ ) and optimized ( $E_{opt}$ ) emissions. Emissions for a shorter period from the TransCom- $CH_4$  experiment (Patra et al., 2011) are also shown for a comparison.

## Variations in global methane sources and sinks during 1910–2010

A. Ghosh et al.

Title Page

Abstract

Introduction

Conclusions

References

Tables

Figures

◀

▶

◀

▶

Back

Close

Full Screen / Esc

Printer-friendly Version

Interactive Discussion

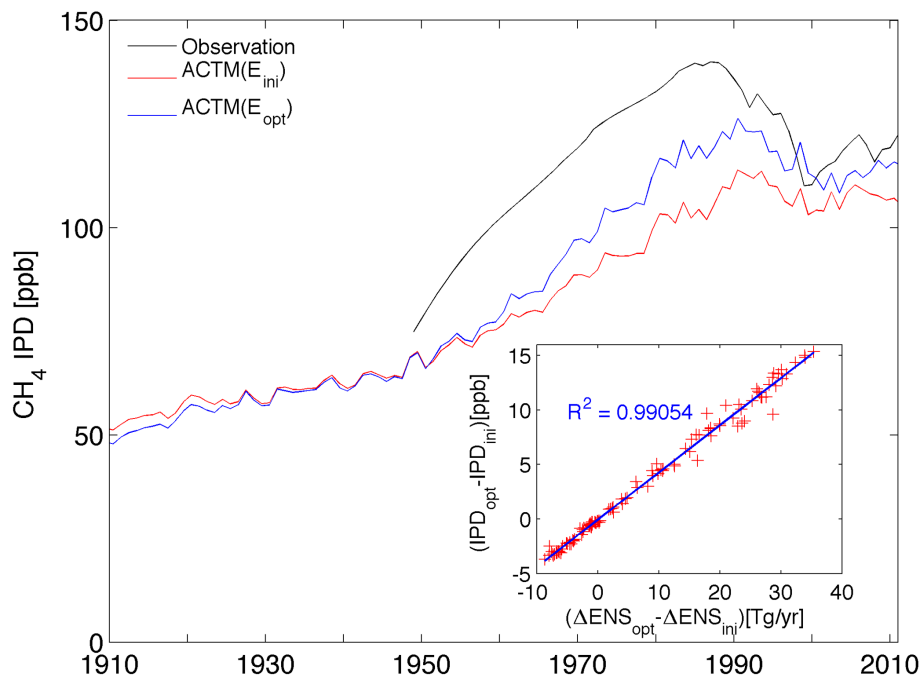


**Figure 5.** Comparison of model simulated and observed inter-polar differences (IPD) of CH<sub>4</sub> concentration. Inset: correlation between difference of IPD (IPD<sub>opt</sub> – IPD<sub>int</sub>) and difference of NH-SH emissions (ΔENS<sub>opt</sub> – ΔENS<sub>int</sub>) in optimized and initial guess cases.

## Variations in global methane sources and sinks during 1910–2010

A. Ghosh et al.

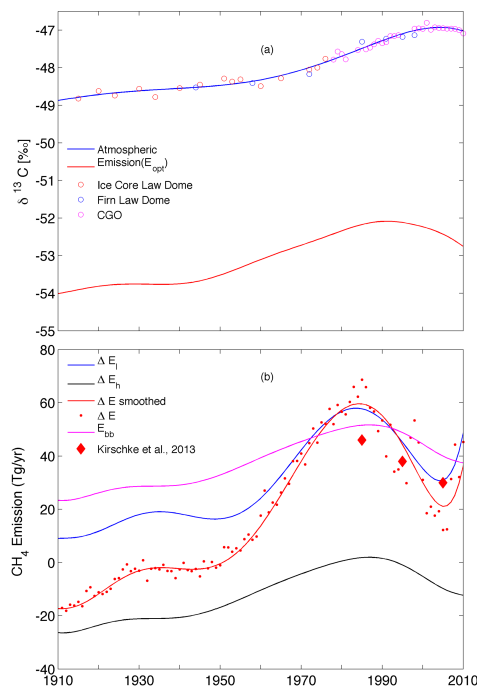


**Figure 6.** (a) Observations (circles) and smooth time series of  $\delta^{13}\text{C}_{\text{atmos}}$  and  $\delta^{13}\text{C}_{\text{Eopt}}$  (b)  $\Delta E$  (smoothed) is split into  $\Delta E_I$  and  $\Delta E_h$ . Here  $\delta^{13}\text{C}_{\Delta E_I}$  and  $\delta^{13}\text{C}_{\Delta E_h}$  are assumed to be  $-60\%$  (biogenic sources, a supplementary source) and  $-21.8\%$  (biomass burning emission), respectively. Annual average  $\delta^{13}\text{C}_{\text{atmos}}$  observations from Law Dome (ice core (red circle)/firn air (blue circle) records) and CGO (air archive samples and NOAA-ESRL network direct observations; (magenta circle)) are shown separately here. The estimated biomass burning emission is given by  $E_{\text{bb}} = 49.7$  (initial biomass burning emission)  $+\Delta E_h$  (correction term)  $\text{Tgyr}^{-1}$ . A recent estimation of biomass burning emissions (Kirschke et al., 2013) for last three decades is also shown for comparison (filled diamond).

[Title Page](#)
[Abstract](#)
[Introduction](#)
[Conclusions](#)
[References](#)
[Tables](#)
[Figures](#)
[Back](#)
[Close](#)
[Full Screen / Esc](#)
[Printer-friendly Version](#)
[Interactive Discussion](#)

## Variations in global methane sources and sinks during 1910–2010

A. Ghosh et al.

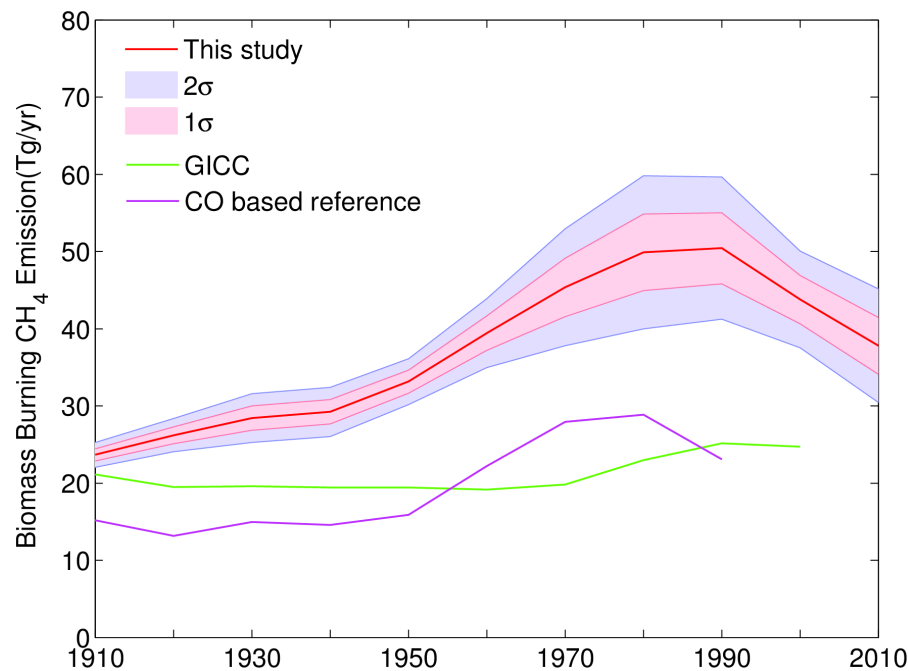


**Figure A1.** Sensitivity of estimated proposed biomass burning emissions with respect to varying  $\delta^{13}\text{C}_{\Delta E_1}$  (biogenic sources) from  $-55$  to  $-65\%$ .

Title Page

Abstract

Introduction

Conclusions

References

Tables

Figures

◀

▶

◀

▶

Back

Close

Full Screen / Esc

Printer-friendly Version

Interactive Discussion

